DOI: 10.1021/ma902378k

Macromolecules
ARTICLE

"Schizophrenic" Self-Assembly of Block Copolymers Synthesized *via* Aqueous RAFT Polymerization: From Micelles to Vesicles†

Adam E. Smith,‡ Xuewei Xu,‡ Stacey E. Kirkland-York,‡ Daniel A. Savin,‡ and Charles L. McCormick*,‡,§

‡*Department of Polymer Science and* §*Department of Chemistry and Biochemistry, The University of Southern Mississippi, Hattiesburg, Mississippi 39406*

Received October 26, 2009; Revised Manuscript Received December 15, 2009

ABSTRACT: Dually responsive poly[(*N*,*N*-diethylaminoethyl methacrylate)-*b*-(*N*-isopropyl acrylamide)]s (P(DEAEMA-*b*-NIPAM)s) capable of "schizophrenic" aggregation in aqueous solution were synthesized via aqueous reversible addition−fragmentation chain transfer (RAFT) polymerization. The nanoassembly morphologies, dictated by the hydrophilic mass fraction, can be controlled by the polymer block lengths, solution pH, and temperature. Both P(DEAEMA$_{98}$-*b*-NIPAM$_{209}$) (52.5 wt % NIPAM) and P(DEAEMA$_{98}$-*b*-NIPAM$_{392}$) (70.8 wt % NIPAM) self-assemble into PDEAEMA-core PNIPAM-shell spherical micelles with a hydrodynamic radii (R_h) of 21 and 25 nm, respectively, at temperatures below the lower critical solution temperature of PNIPAM and at solution pH values greater than the pK_a of PDEAEMA. The two block copolymers, however, display quite different temperature-responsive behaviors at pH < 7.5. At elevated temperatures (>42 °C) P(DEAEMA$_{98}$-*b*-NIPAM$_{209}$) forms spherical micelles (R_h = 28 nm) with hydrophobic PNIPAM cores stabilized by a hydrophilic PDEAEMA shell. By contrast, P(DEAEMA$_{98}$-*b*-NIPAM$_{392}$) assembles into vesicles (R_h = 99 nm) above 38 °C. The nanostructures were characterized by a combination of dynamic and static light scattering as well as transmission electron microscopy and are being investigated for their potential application as drug delivery vehicles.

Introduction

Self-assembly of block copolymers with precisely defined structures is the subject of intensive research for applications in nanomedicine. Micelles formed from amphiphilic block copolymers in aqueous solution, for example, have been investigated in recent years as potential carriers for therapeutic and diagnostic agents.[1] Micelles are not, however, the only structures formed from self-assembling amphiphilic block copolymers, rather they are part of a morphological continuum that includes worm-like micelles and polymeric vesicles (commonly referred to as polymersomes in comparison to liposomes).[2−4] While micelles are generally limited to the entrapment of hydrophobic drugs within their hydrophobic cores, polymersomes can simultaneously "capture" hydrophobic and hydrophilic species due to the presence of a hydrophobic lamellar wall and an internal aqueous compartment of these synthetic vesicles.[5] Additionally, polymersomes exhibit increased stability, greater storage capacity, and prolonged circulation time compared to liposomes.[6]

Discher and Eisenberg have developed an empirical relationship between the block copolymer composition and the self-assembled morphology.[7] Spherical micelles are expected for polymers with hydrophilic mass fractions (*f*) greater than 45%, while copolymers with $f \approx 35 \pm 10\%$ typically assemble into polymersomes. A number of reviews have been published describing the correlation between the hydrophilic mass fraction and the resulting solution morphology.[7−9] Recently, Sundararaman and Grubbs synthesized a poly(ethylene oxide)-*b*-poly(*N*-isopropyl acrylamide)-*b*-poly(isoprene) (PEO-*b*-PNIPAM-*b*-PI) triblock copolymer and investigated the aqueous solution morphology above and below the LCST of the PNIPAM block.[10] At room temperature, the triblock copolymers aggregate into spherical micelles with PI cores. After 4 weeks at 65 °C, a temperature at which the PNIPAM block is hydrophobic, the aggregate morphology shifted to form vesicles. The morphological change was attributed to the alteration of the hydrophobic/hydrophilic ratio above and below the LCST of PNIPAM. Zhao and co-workers studied the effect of copolymer composition, concentration, and heating rate on the size and the morphology of PEO and NIPAM copolymers.[11] Recently, we reported the ability to tune the solution morphology of a series of poly[(*N*,*N*-dimethylaminoethyl methacrylate)-*b*-(*N*-isopropyl acrylamide)]s (P(DMAEMA-*b*-NIPAM)s) using composition, solution pH, temperature, and ionic strength to control the hydrophilic mass fraction.[12]

The ability to synthesize block copolymers with tunable hydrophilicity by the incorporation of stimuli-responsive blocks provides a valuable tool for the verification of the empirical relationship between hydrophilic mass fraction and the resulting solution morphology. With the emergence of CRP techniques such as nitroxide-mediated polymerization (NMP),[13] atom transfer radical polymerization (ATRP),[14] and reversible addition−fragmentation chain transfer polymerization (RAFT),[15] researchers are now capable of synthesizing the well-defined (co)polymers with advanced architectures, including block copolymers, without the stringent reaction conditions required for anionic polymerizations. Additionally, the CRP polymerization methods, RAFT in particular, enable the incorporation of a wide variety of functionalities. As such, great effort has been directed toward investigating the synthesis and assembly of stimuli-responsive block copolymers directly in aqueous media.[16,17] Included in this effort is the synthesis of block copolymers incorporating two or more responsive blocks which can form

† Paper number 143 in a series on Water-Soluble Polymers.

*To whom correspondence should be addressed. E-mail: Charles.McCormick@usm.edu.

 Published on Web 01/11/2010

Scheme 1. Representation or Proposed "Schizophrenic" Aggregation Behavior for (a) P(DEAEMA$_{98}$-*b*-NIPAM$_{209}$) and (b) P(DEAEMA$_{98}$-*b*-NIPAM$_{392}$)

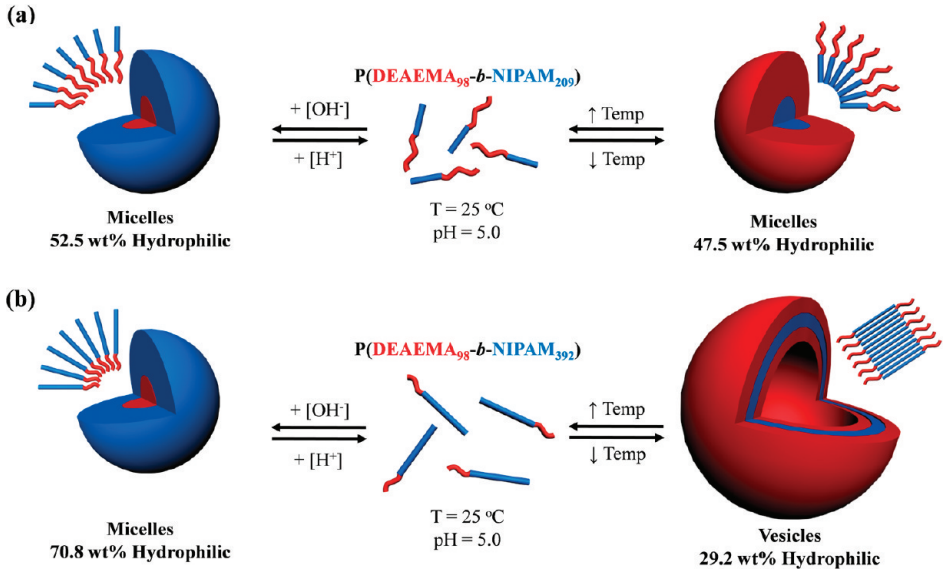

two distinct structures using external stimuli (temperature, pH, salt, etc.). Armes and co-workers coined the term "schizophrenic" micellization to describe these systems.[18] Since the initial report of "schizophrenic" diblock copolymers,[19] a number of systems have been described using dual pH-responsive blocks,[19−25] dual thermoresponsive blocks,[26−28] dual salt-responsive blocks,[29] a pH- and a temperature-responsive block,[30−37] and a pH- and a salt-responsive block.[38]

Herein, we report the synthesis and solution behavior of two poly[(*N*,*N*-diethylaminoethyl methacrylate)-*b*-*N*-isopropylacrylamide]s (P(DEAEMA-*b*-NIPAM)s) specifically designed utilizing the empirical relationship between hydrophilic mass fraction and the resulting solution morphology. By adjusting the pH and temperature, PDEAEMA and PNIPAM blocks were respectively rendered hydrophobic. Aqueous RAFT polymerization was utilized to ensure the synthesis of well-defined block copolymers with narrow PDIs. We describe the first example, to our knowledge, of double hydrophilic block copolymers exhibiting a morphological transition from micelles to vesicles based on stimuli-responsive behavior.

Experimental Section

Materials. All reagents were purchased from Aldrich at the highest purity available and used as received unless otherwise stated. 4,4-Azobis(4-cyanopentanoic acid) (V-501) and 4,4′-Azobis[2-(imidazolin-2-yl)propane] dihydrochloride (VA-044) were donated by Wako Chemicals and were recrystallized twice from methanol prior to use. NIPAM was recrystallized twice from hexanes prior to use. DEAEMA was dried with CaH_2 and vacuum distilled prior to use. 4-Cyano-4-(ethylsulfanylthiocarbonyl) sulfanylpentanoic acid (CEP) was synthesized according to a previous literature procedure.[39]

General Procedure for the Aqueous RAFT Polymerization of DEAEMA. A solution of CEP (71.0 mg, 0.270 mmol), DEAEMA (5.0 g, 0.027 mol), and V-501 (15.1 mg, 0.054 mmol) in 10 mL of deionized water was added to a 50 mL round-bottom flask. Concentrated HCl was added to the solution to lower the pH to 4.5 to ensure the PDEAEMA polymer remained soluble. The solution was then sparged with nitrogen for approximately 30 min, and the flask was placed in a preheated oil bath at 70 °C. The reaction was terminated after 8 h by quenching the reaction tube in liquid nitrogen followed by exposure to air. The product was purified by dialysis against DI water (pH 4.5) for 3 days followed by lyophilization.

Block Copolymer Synthesis. The PDEAEMA$_{98}$-CEP macroCTA was chain extended with NIPAM to yield two diblock copolymers following a similar procedure. For example, NIPAM (1.7 g, 10.6 mmol), PDMAEMA$_{98}$ (1.0 g), and VA-044 (17.6 mg, 0.054 mmol) were dissolved in 6 mL of DI water and added to a 25 mL round-bottom flask. After sparging with nitrogen for 30 min, the reaction was allowed to proceed at 25 °C for 12 h. The reaction mixture was then quenched by cooling the reaction vessel in liquid nitrogen and exposure to air. The product was purified by dialysis against DI water (pH 4.5) for 3 days followed by lyophilization.

Self-Assembly of P(DEAEMA$_{98}$-*b*-NIPAM$_x$). Copolymers were dissolved directly in deionized water at a concentration of 0.01 wt % (0.1 mg/mL). For temperature-induced assembly, the pH was adjusted to 5.0 using 0.1 N HCl or 0.1 N NaOH, and the temperature was slowly increased to 50 °C (1 °C/min).

Size Exclusion Chromatography (SEC). SEC was used to determine the number-average molecular weight (M_n) and polydispersity indices (PDIs) for the PDEAEMA homopolymer and the block copolymers of DEAEMA and NIPAM. The PDEAEMA macroCTA was analyzed by aqueous size exclusion chromatography (ASEC) using an aqueous eluent of 1.0 wt % acetic acid/0.1 M Na_2SO_4. A flow rate of 0.25 mL/min, Eprogen Inc. columns [CATSEC1000 (7 μ, 50 × 4.6), CATSEC100 (5 μ, 250 × 4.6), CATSEC1000 (7 μ, 250 × 4.6) and CATSEC300 (5 μ, 250 × 4.6)], a Wyatt Dawn EOS multiangle laser light scattering detector (λ = 690 nm), and an Optilab DSP interferometric refractometer (λ = 690 nm) were used. Wyatt DNDC for Windows was used for the PDEAEMA dn/dc determination. The PDEAEMA macroCTA and the two P(DEAEMA-*b*-NIPAM)s were analyzed using a DMF eluent (0.02 M LiBr) at a flow rate of 1.0 mL/min in combination with Viscotek I-Series Mixed Bed low-MW and mid-MW columns and a Viscotek-TDA 302 (RI, viscosity, 7 mW 90° and 7° true low angle light scattering detectors (670 nm)) at 35 °C. The dn/dc of each (co)polymer was determined in DMF at 35 °C using a Viscotek refractometer and Omnisec software.

^{1}H NMR Spectroscopy. ^{1}H NMR measurements were performed with a temperature-controlled Varian UNITY INOVA spectrometer operating at a frequency of 499.8 MHz. Samples were prepared in D_2O (HOD internal standard), and spectra were recorded for each copolymer at temperatures of 25 and

Scheme 2. Synthesis of Dually Responsive Block Copolymers of DEAEMA and NIPAM *via* Aqueous RAFT Polymerization

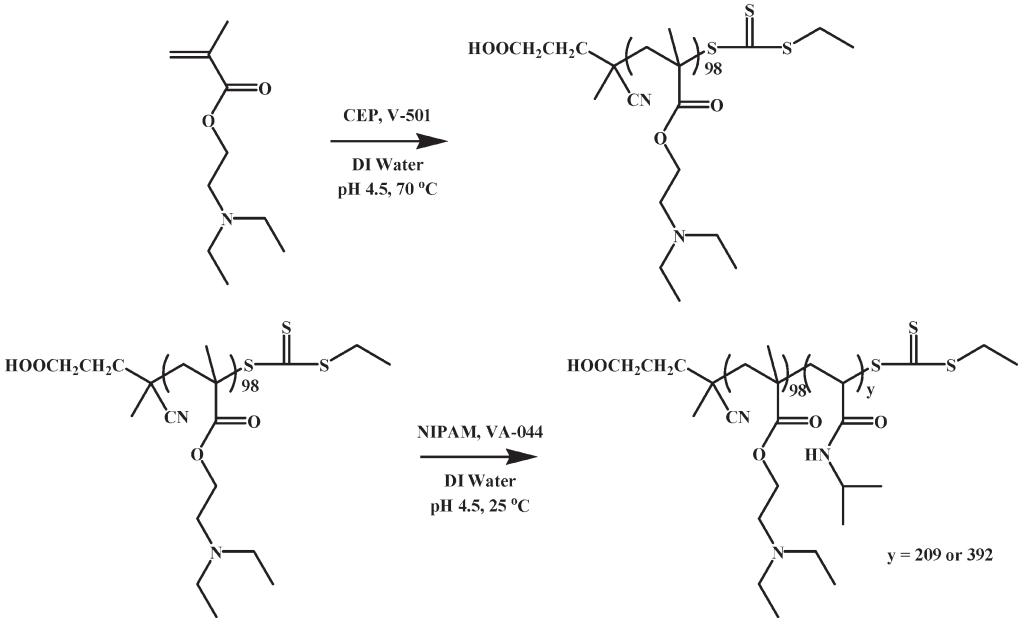

50 °C and pD values of 5.0 and 9.0. Block copolymer compositions were determined by comparing resonances of the PDEAEMA block to those associated with the PNIPAM block in the spectra recorded at 25 °C.

Light Scattering. Dynamic light scattering (DLS) studies investigating the effect of incremental temperature and pH changes were conducted using a Malvern Instruments Zetasizer Nano series instrument equipped with a 4 mW He−Ne laser operating at $\lambda = 632.8$ nm, an avalanche photodiode detector with high quantum efficiency, and an ALV/LSE-5003 multiple tau digital correlator electronics system. Dispersion Technology Software 5.03 (Malvern Instruments) was used to record and analyze the data to determine particle size distributions.

Variable-angle DLS and SLS measurements were made using incident light at 633 nm from a Spectra Physics HeNe laser operating at 40 mW. The angular dependence of the autocorrelation functions was measured using a Brookhaven Instruments BI-200SM goniometer with an avalanche photodiode detector and TurboCorr correlator. Correlation functions were analyzed according to the method of cumulants using the companion software. All data reported correspond to the average decay rate obtained from the second cumulant fit. Apparent diffusion coefficients (D_{app}) were obtained from the slope of the relaxation frequency (Γ) versus q^2 where

$$q = \frac{4\pi n}{\lambda}\sin\left(\frac{\theta}{2}\right) \quad (1)$$

λ is the wavelength of the incident laser (633 nm), θ is the scattering angle, and n is the refractive index of the media. The hydrodynamic radius (R_h) was then calculated from the Stokes−Einstein equation (eq 2)

$$R_h = \frac{k_B T}{6\pi\eta D_{app}} \quad (2)$$

where k_B is the Boltzmann constant, T is the temperature, and η is the viscosity of the medium.

Angular-dependent static light scattering (SLS) experiments were performed on aqueous polymer solutions with the same instrument as described above. The radius of gyration (R_g) of the assemblies was determined from the angular dependence of the scattering intensity. A Zimm plot of the scattering intensity (I_{ex}) versus the square of the scattering vector (q) was used to determine the radius of gyration (R_g). A Berry plot ($I_{ex}^{-1/2}$ vs q^2) is used in instances where a Zimm treatment results in upward curvature of the data when $qR_g \geq 1$.

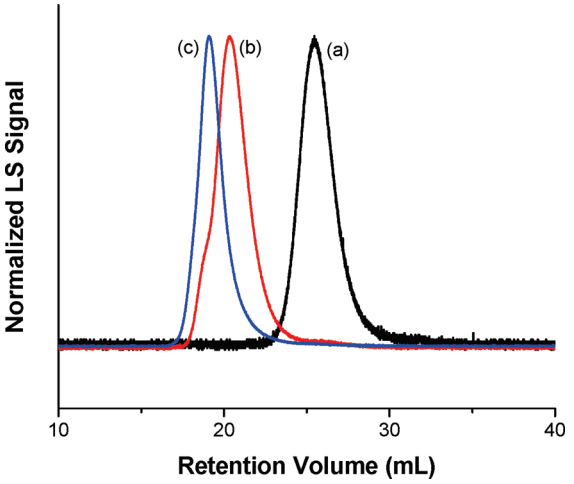

Figure 1. SEC chromatograms for (a) $PDEAEMA_{98}$, (b) P(DEAEMA$_{98}$-*b*-NIPAM$_{209}$), and (c) P(DEAEMA$_{98}$-*b*-NIPAM$_{392}$).

Solutions were prepared by dissolving the polymer into purified water to a concentration of 0.01 wt %. Samples were agitated to ensure complete dissolution and then filtered through a 0.45 μm PVDF syringe-driven filter (Millipore) directly into the scattering cell. Samples were then sonicated and allowed to reach thermal equilibrium prior to measurements.

Transmission Electron Microscopy (TEM). Transmission electron microscopy measurements were conducted using a JEOL JEM-2100 electron microscope at an accelerating voltage of 200 kV. The specimens were prepared by placing a 5 μL drop of the nanostructure solution on a carbon-coated copper grid followed by water evaporation at either 25 or 50 °C. The grids were subsequently stained using a 1 wt % phosphotungstic acid solution which stained the amino functionality of DEAEMA.[40]

Table 1. Summary of P(DEAEMA$_{98}$-*b*-NIPAM$_x$) Molecular Weights and Compositions

	M_n (kDa)[a]	PDI[a]	wt% (mol %) NIPAM [a]	wt% (mol %) NIPAM [b]
PDEAEMA$_{98}$	18.4	1.07	–	–
P(DEAEMA$_{98}$-*b*-NIPAM$_{209}$)	39.3	1.08	53.4 (65.4)	52.5 (64.4)
P(DEAEMA$_{98}$-*b*-NIPAM$_{392}$)	63.9	1.10	71.4 (80.4)	72.4 (81.1)

[a] As determined by SEC. [b] As determined by ^{1}H NMR.

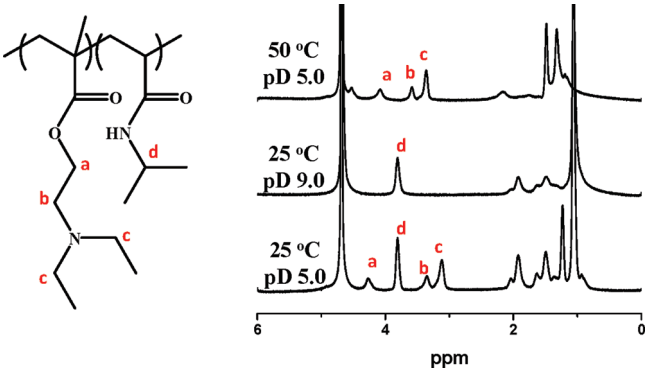

Figure 2. ^{1}H NMR spectra of P(DEAEMA$_{98}$-*b*-NIPAM$_{209}$) (0.1 wt % in D_2O) at (A) 25 °C and pD 5.0, (B) 25 °C and pD 9.0, and (C) 50 °C and pD 5.0.

Results and Discussion

Synthesis of Block Copolymers of DEAEMA and NIPAM. RAFT provides a facile technique for preparing well-defined amphiphilic diblock copolymers of preselected compositions to test the effect of block lengths (i.e., hydrophilic weight fraction) on the self-assembled morphology in aqueous solution. The present diblock copolymer system was chosen due to the pH-response of PDEAEMA (p$K_a \sim 7.3$)[41] and the thermoresponse of PNIPAM (LCST $\approx$ 32 °C). Specific copolymer compositions were targeted to produce hydrophilic mass fractions for "schizophrenic" micelle-to-unimer-to-micelle (Scheme 1A) and micelle-to-unimer-to-vesicle (Scheme 1B) transitions according to Discher's and Eisenberg's empirical relationship.[7] The diblock copolymers of DEAEMA and NIPAM were synthesized according to Scheme 2. The trithiocarbonate, CEP, was used to mediate the aqueous RAFT polymerization of DEAEMA in the presence of the free radical initiator V-501 to yield PDEAEMA$_{98}$ (M_n = 18.4 kDa, PDI = 1.07). The PDEAEMA$_{98}$ macroCTA was subsequently chain extended with NIPAM to produce two diblock copolymers. The diblock copolymers were targeted to have 50 and 70 wt % NIPAM. The two diblock copolymers, P(DEAEMA$_{98}$-*b*-NIPAM$_{209}$) (M_n = 39.3 kDa, PDI = 1.08) and P(DEAEMA$_{98}$-*b*-NIPAM$_{392}$) (M_n = 63.9 kDa, PDI = 1.10), were determined to have 53.4 and 71.4 wt % NIPAM, respectively, using SEC (Figure 1). ^{1}H NMR studies of the two diblock copolymers revealed weight fractions (52.5 and 70.8 wt %) in agreement with those determined by SEC. SEC chromatograms of PDEAEMA$_{98}$, P(DEAEMA$_{98}$-*b*-NIPAM$_{209}$), and P(DEAEMA$_{98}$-*b*-NIPAM$_{392}$) were unimodal, and the PDIs were low (< 1.2)

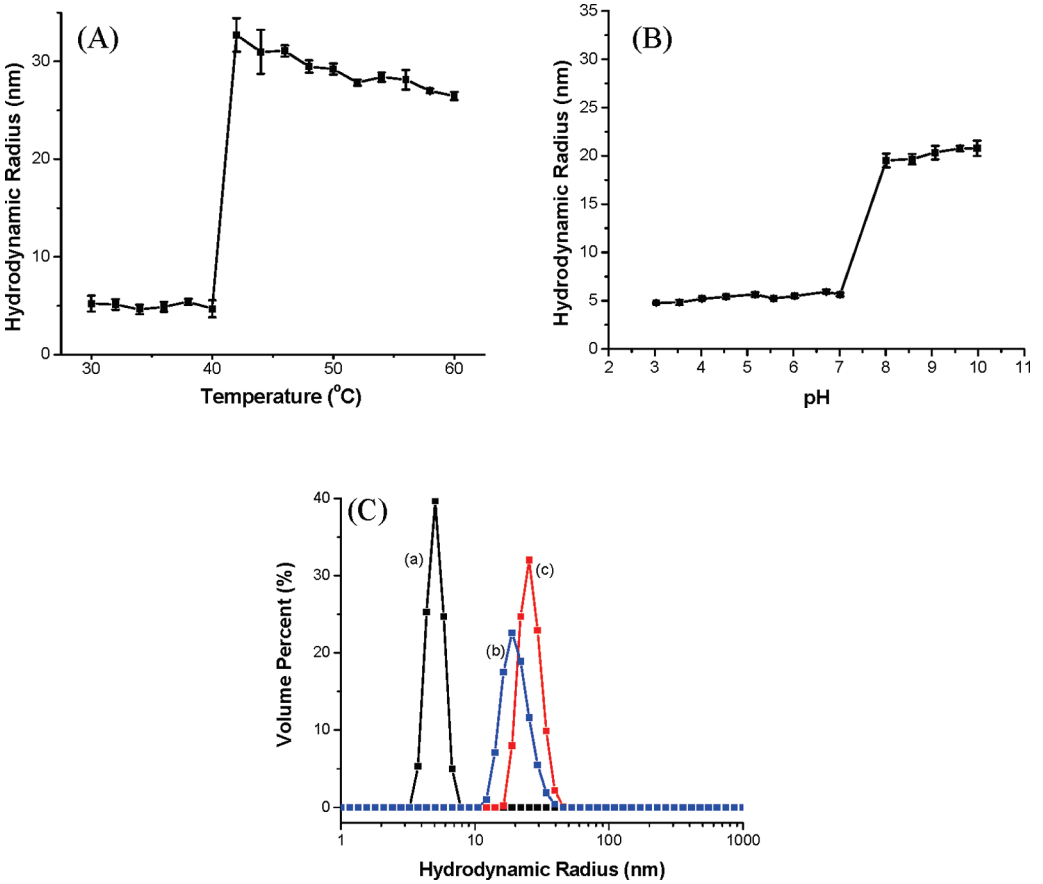

Figure 3. (A) Temperature- and (B) pH-responsive aggregation behavior of P(DEAEMA$_{98}$-*b*-NIPAM$_{209}$) (0.01 wt %) at (●) 25 °C and variable pH and (■) pH 5.0 and variable temperature. (C) Hydrodynamic radius of P(DEAEMA$_{98}$-*b*-NIPAM$_{209}$) (0.01 wt %) at (a) 25 °C and pH 5.0, (b) 25 °C and pH 9.0, and (c) 50 °C and pH 5.0.

indicating near-quantitative blocking efficiency and controlled polymerization. The molecular weight and composition data of the diblock copolymer series are summarized in Table 1.

"Schizophrenic" Self-Assembly of P(DEAEMA$_{98}$-*b*-NIPAM$_{209}$). Block copolymers of DEAEMA and NIPAM are expected to undergo "schizophrenic" aggregation behavior due to the separate responsive behaviors exhibited by the two blocks. ^{1}H NMR was utilized to investigate the dual responsiveness of the two P(DEAEMA-*b*-NIPAM)s in aqueous solution. Figure 2 shows the temperature- and pD-dependent ^{1}H NMR spectra for P(DEAEMA$_{98}$-*b*-NIPAM$_{209}$) (0.01 wt %) dissolved in D_2O. At 25 °C and pD 5.0, the diblock copolymers are expected to exist as unimers, since the conditions are below the pK_a of the PDEAEMA block and below the LSCT of the PNIPAM block. In the ^{1}H NMR spectrum of Figure 2A, the characteristic resonances of PDEAEMA (a, b, and c) and the characteristic resonance of PNIPAM (d) are readily visible. Increasing the pD to a value of 9.0 leads to deprotonation and hydrophobic collapse of the PDEAEMA block, as evidenced by the attenuation of peaks a, b, and c associated with PDEAEMA while the PNIPAM peak d is still present. Conversely, at 50 °C and pD 5.0, the peak for the PNIPAM is attenuated and the PDEAEMA peaks are seen. While the ^{1}H NMR experiments provide evidence for the "schizophrenic" self-assembly behavior, conclusions as to the aggregate morphology cannot be made from these data.

The stimuli-responsive behavior of P(DEAEMA$_{98}$-*b*-NIPAM$_{209}$) was additionally investigated using DLS. Figure 3A and 3B show the temperature- and pH-responsiveness of P(DEAEMA$_{98}$-*b*-NIPAM$_{209}$) (0.01 wt %) in aqueous solution, respectively. Measurements were conducted at 25 °C, well below the LCST of PNIPAM, ensuring its hydrophilicty. Under these conditions, P(DEAEMA$_{98}$-*b*-NIPAM$_{209}$) exists as unimers ($R_h \approx 5$ nm) (Figure 3C, curve a). At pH values above the pK_a of PDEAEMA, P(DEAEMA$_{98}$-*b*-NIPAM$_{209}$) self-assembles into aggregates with hydrodynamic radii of ~20 nm (Figure 3C, curve b). To ensure the PDEAEMA block remains protonated, and therefore hydrophilic, the thermoresponsive self-assembly of P(DEAEMA$_{98}$-*b*-NIPAM$_{209}$) was studied at a solution pH of 5.0. At temperatures above 42 °C, this diblock copolymer formed aggregates with radii between 25 and 32 nm. The size of these aggregates decreased with increasing temperature above the critical aggregation temperature (CAT) which can be attributed to increasing dehydration of the PNIPAM block.[42,43] At 50 °C, P(DEAEMA$_{98}$-*b*-NIPAM$_{209}$) formed aggregates of 26.1 nm (Figure 3C, curve c). While DLS at a single angle allows for determination of the hydrodynamic size of the nanoassemblies, it does not provide information on aggregate morphology.

To study the nature of the aggregate structure, variable angle DLS and SLS were used in combination with electron microscopy. The angular dependent DLS and SLS results for aggregates formed from P(DEAEMA$_{98}$-*b*-NIPAM$_{209}$) at 25 °C and pH 9.0 are shown in Figure 4A. A plot of the relaxation frequency (Γ) versus the square of the scattering vector (q^2) gives a linear relationship, indicative of Brownian diffusion of spherical particles. The slope through the origin yields a diffusion coefficient of 1.153×10^{-11} m^2/s. Using the Stokes−Einstein equation (eq 2), an apparent R_h of 21.2 nm was determined, which is in good agreement with measurements taken at a fixed angle. A radius of gyration (R_g) of 16.4 nm was calculated using a Zimm treatment of the SLS data. The ratio of R_g/R_h determined from angular dependent DLS and from SLS for the self-assembled aggregates of P(DEAEMA$_{98}$-*b*-NIPAM$_{209}$) at 25 °C and pH 9.0 is 0.774,

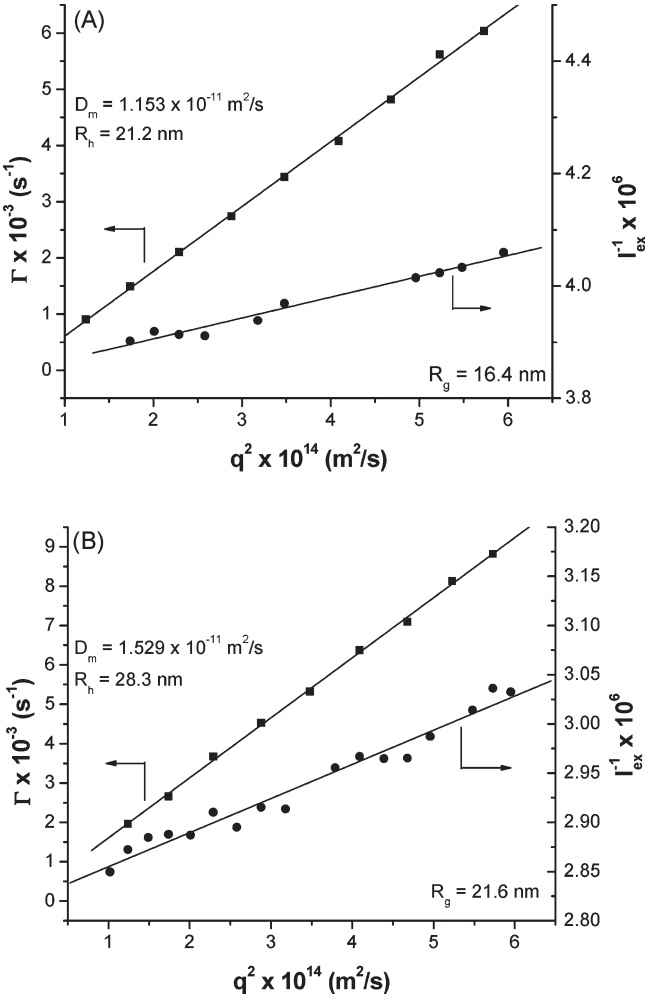

Figure 4. Angular dependent DLS (■) and SLS (●) measurements performed on P(DEAEMA$_{98}$-*b*-NIPAM$_{209}$) (0.01 wt %) at (A) 25 °C and pH 9.0 and (B) 50 °C and pH 5.0.

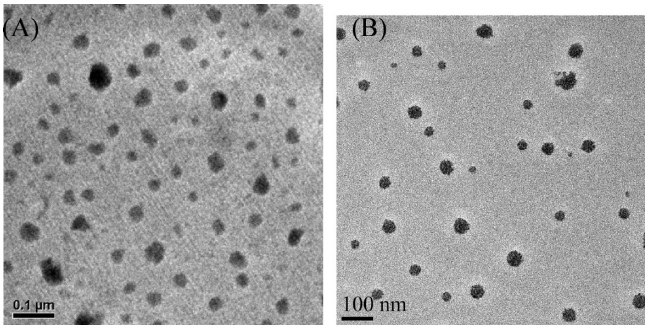

Figure 5. TEM micrographs of P(DEAEMA$_{98}$-*b*-NIPAM$_{209}$) (0.01 wt %) at (a) 25 °C and pH 9.0 and (b) 50 °C and pH 5.0.

which is indicative of hard-sphere particles.[44−46] The formation of spherical particles at 25 °C and pH 9.0 was also confirmed by TEM (Figure 5A). By utilizing a combination of techniques (^{1}H NMR, light scattering, and TEM), the aggregate morphology of each system has been elucidated. P(DEAEMA$_{98}$-*b*-NIPAM$_{209}$) self-assembles into PDEAEMA-core, PNIPAM-shell spherical micelles at 25 °C and pH 9.0. Furthermore, LS experiments of P(DEAEMA$_{98}$-*b*-NIPAM$_{209}$) at 50 °C and pH 5.0 (Figure 4B) indicated R_h, R_g, and R_g/R_h values of 28.3 nm, 21.6 nm, and 0.763, respectively (Table 2). These values along with ^{1}H NMR (Figure 2C) and TEM (Figure 5B) measurements support the

formation of PNIPAM-core, PDEAEMA-shell spherical micelles.

"Schizophrenic" Morphological Assembly of P(DEAEMA$_{98}$-*b*-NIPAM$_{392}$). The second diblock copolymer, P(DEAEMA$_{98}$-*b*-NIPAM$_{392}$), was designed such that the self-assembly into micelles would occur under conditions rendering the PDEAEMA block hydrophobic and vesicles when the PNIPAM block was hydrophobic. Fixed angle DLS was used to study the effects of solution pH and temperature on the size of the self-assembled aggregates. As observed for P(DEAEMA$_{98}$-*b*-NIPAM$_{209}$), a plot of hydrodynamic size versus solution pH (Figure 6B) revealed a transition from unimers ($R_h \approx 7$ nm) (Figure 6C, curve a) to aggregates with radii of ~26 nm above the pK_a of PDEAEMA at 25 °C (Figure 6C, curve b). The temperature-responsive self-assembly of P(DEAEMA$_{98}$-*b*-NIPAM$_{392}$) was analyzed at pH 5.0 to ensure that the PDEAEMA segments remained hydrophilic. The CAT of P(DEAEMA$_{98}$-*b*-NIPAM$_{392}$) is 38 °C (Figure 6A), which is lower than that observed for P(DEAEMA$_{98}$-*b*-NIPAM$_{209}$). This has been attributed to the increased hydrophobic content in the diblock copolymer.[47,48] At 38 °C, P(DEAEMA$_{98}$-*b*-NIPAM$_{392}$) self-assembled into aggregates with an apparent R_h of 108 nm. The size of the aggregates decreased with increasing temperature as observed for the micelles formed from P(DEAEMA$_{98}$-*b*-NIPAM$_{209}$) above the CAT. At 50 °C, P(DEAEMA$_{98}$-*b*-NIPAM$_{392}$) self-assembles into aggregates with an R_h of 98.8 nm (Figure 6C, curve c).

Angular dependent DLS and SLS were also utilized to investigate the observed morphology of P(DEAEMA$_{98}$-*b*-NIPAM$_{392}$) under various solution conditions. At temperatures below the LCST of PNIPAM, when the pH is increased above the pK_a of PDEAEMA, the diblock copolymer is 70.8 wt % hydrophilic and should aggregate to form spherical micelles according to the empirical relationship proposed by Discher and Eisenberg.[7] Figure 7A shows the LS analysis of P(DEAEMA$_{98}$-*b*-NIPAM$_{392}$) at 25 °C and a solution pH of 9.0 (Table 3). Multiangle DLS measurements yield an apparent diffusion coefficient and an R_h value of 9.625×10^{-12} m^2/s and 25.4 nm, respectively. An R_g of 21.1 nm is measured using SLS yielding an R_g/R_h value of 0.793, indicative of spherical micelles.[44−46] TEM also confirms the formation of spherical micelles (Figure 8A) from P(DEAEMA$_{98}$-*b*-NIPAM$_{392}$) at 25 °C and a solution pH value of 9.0. When the solution pH is maintained at 5.0 to ensure that PDEAEMA is hydrophilic, the solution temperature can be raised above the LCST of PNIPAM to induce self-assembly. Under these conditions, P(DEAEMA$_{98}$-*b*-NIPAM$_{392}$) has a hydrophilic mass fraction of 29.2 wt % and should self-assemble into vesicles. Angular-dependent DLS and SLS reveal apparent R_h and R_g values of 91.4 and 99.2 nm, respectively. The ratio of R_g/R_h (1.08) corresponds well to the theoretical

Table 2. Summary of Light Scattering Data for P(DEAEMA$_{98}$-*b*-NIPAM$_{209}$)

pH	T (°C)	R_g [b] (nm)	R_h [a] (nm)	R_h [b] (nm)	R_g/R_h [a]	R_g/R_h [b]
5.0	25		5.1			
9.0	25	16.4	20.6	21.2	0.796	0.774
5.0	50	21.6	26.1	28.3	0.828	0.763

[a] Measured using Malvern Instruments Zetasizer Nano. [b] Measured using a Spectra Physics Millenia laser in conjunction with a Brookhaven Instruments BI-200SM goniometer and TurboCorr correlator.

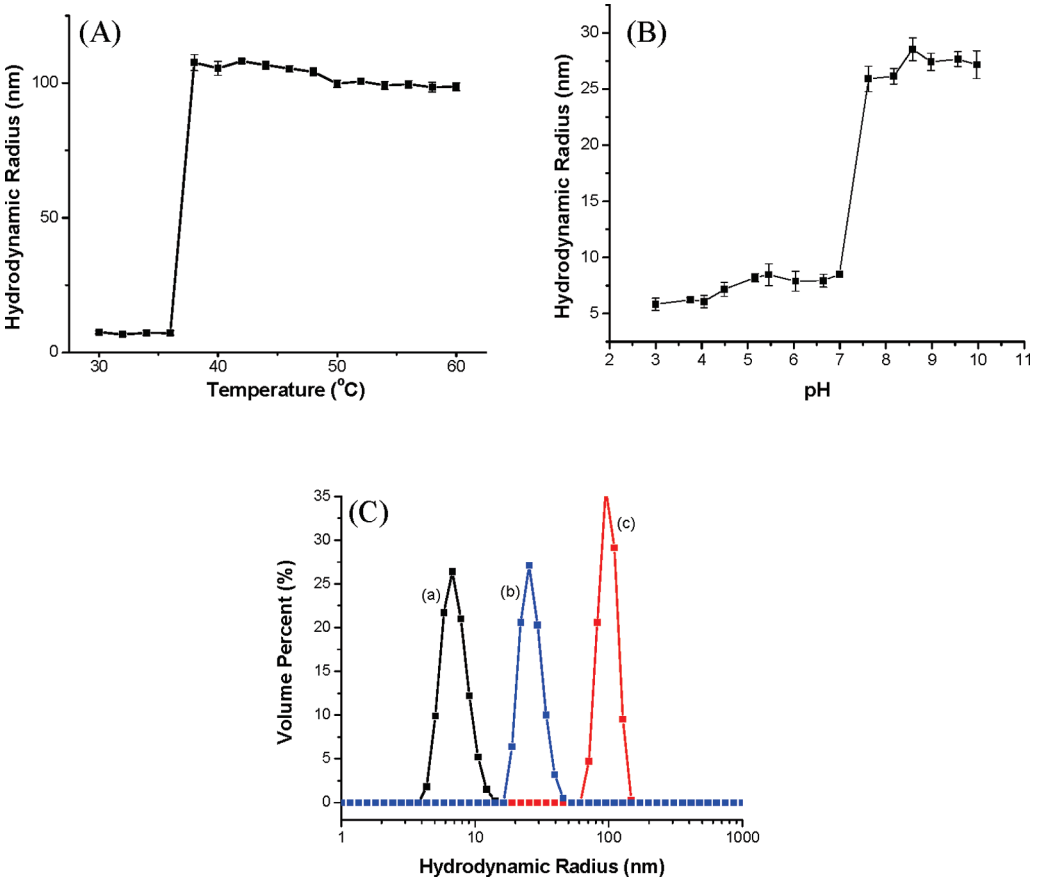

Figure 6. (A) Temperature- and (B) pH-responsive aggregation behavior of P(DEAEMA$_{98}$-*b*-NIPAM$_{392}$) (0.01 wt %) at (●) 25 °C and variable pH and (■) pH 5.0 and variable temperature. (B) Hydrodynamic radius of P(DEAEMA$_{98}$-*b*-NIPAM$_{392}$) (0.01 wt %) at (a) 25 °C and pH 5.0, (b) 25 °C and pH 9.0, and (c) 50 °C and pH 5.0.

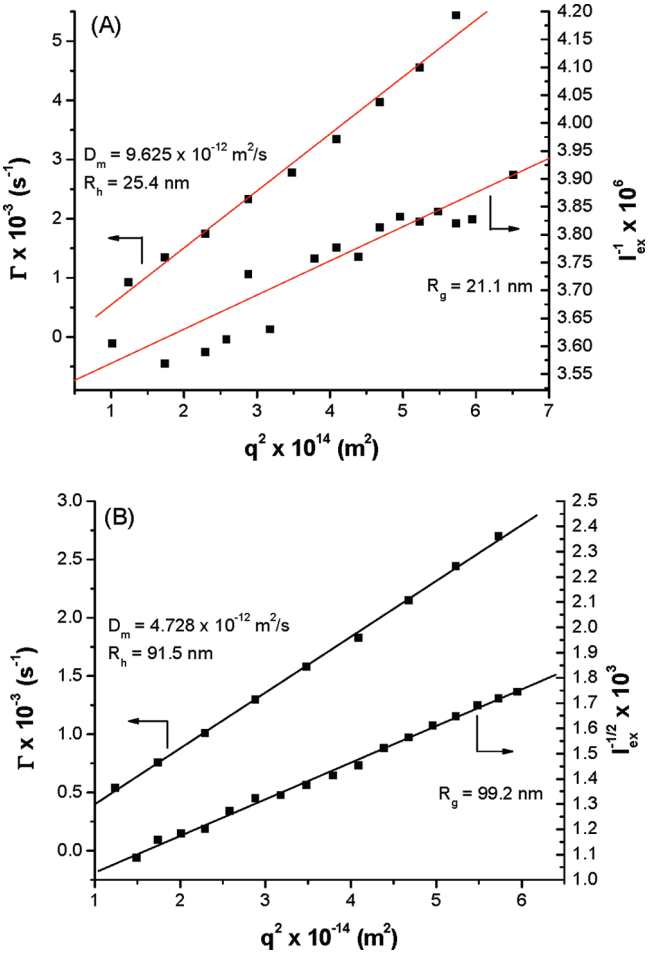

Figure 7. Angular dependent DLS (■) and SLS (●) measurements performed on P(DEAEMA$_{98}$-*b*-NIPAM$_{392}$) (0.01 wt %) at (A) 25 °C and pH 9.0 and (B) 50 °C and pH 5.0.

Table 3. Summary of Light Scattering Data for P(DEAEMA$_{98}$-*b*-NIPAM$_{392}$)

pH	*T* (°C)	R_g [b] (nm)	R_h [a] (nm)	R_h [b] (nm)	R_g/R_h [a]	R_g/R_h [b]
5.0	25		7.2			
9.0	25	21.1	26.6	25.4	0.793	0.831
5.0	50	99.2	98.8	91.4	1.00	1.08

[a] Measured using Malvern Instruments Zetasizer Nano. [b] Measured using a Spectra Physics Millenia laser in conjunction with a Brookhaven Instruments BI-200SM goniometer and TurboCorr correlator.

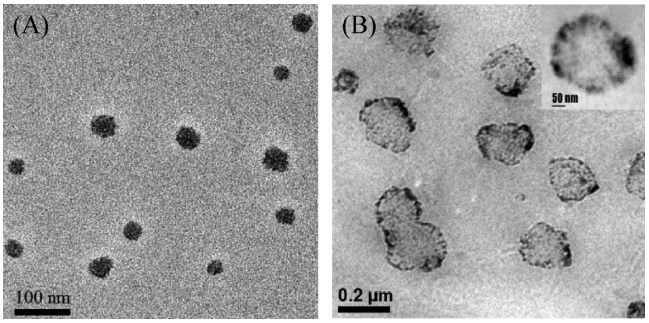

Figure 8. TEM micrographs of P(DEAEMA$_{98}$-*b*-NIPAM$_{392}$) (0.01 wt %) at (a) 25 °C and pH 9.0 and (b) 50 °C and pH 5.0.

value for vesicles (1.0).[44–46] TEM micrographs of samples stained with phosphotungstic acid confirm structures with the characteristic vesicular structure (Figure 8B). Note that the Γ vs q^2 plots remain linear, indicating that the spherical morphology is retained over the pH and temperature range.

Conclusions

The aqueous RAFT synthesis and characterization of dually responsive diblock copolymers of DEAEMA and NIPAM capable of "schizophrenic" aggregation into multiple morphologies are described. The two diblock copolymers were specifically designed according to the empirical relationship proposed by Discher and Eisenberg[7] correlating the hydrophilic mass fraction to the resultant self-assembled solution morphology. The smaller block copolymer, P(DEAEMA$_{98}$-*b*-NIPAM$_{209}$) (52.5 wt % NIPAM), assembled into (a) spherical PDEAEMA-core micelles below the LCST of PNIPAM and above the pK_a of PDEAEMA and (b) spherical PNIPAM-core micelles above the LCST of PNIPAM and below the pK_a of PDEAEMA. The larger block copolymer, P(DEAEMA$_{98}$-*b*-NIPAM$_{392}$) (70.8 wt % PNIPAM), was designed to be asymmetric and capable of assembly into micelles at high pH and vesicles at high temperature. At 25 °C and pH > 7.5, P(DEAEMA$_{98}$-*b*-NIPAM$_{392}$) was shown to assemble into PDEAEMA-core micelles, whereas, at pH 5.0 and temperatures above the CAT, vesicles were formed. To our knowledge, this represents the first report of a block copolymer system capable of a "schizophrenic" micelle-to-unimer-to-vesicle morphological transition in aqueous solution in response to multiple stimuli.

Acknowledgment. The Department of Energy (DE-FC26-01BC15317), MRSEC program of the National Science Foundation (NSF) (DMR-0213883), and the Robert M. Hearin Foundation are gratefully acknowledged for financial support. The authors also acknowledge the NSF Division of Materials Research/Major Research Instrumentation Awards 0079450 and 0421406 for the purchase of the Varian Unity Inova 500 MHz NMR spectrometer and JEOL JEM-2100 electron microscope.

References and Notes

(1) York, A. W.; Kirkland, S. E.; McCormick, C. L. *Adv. Drug Delivery Rev.* **2008**, *60*, 1018–1036.
(2) Zhang, L. F.; Eisenberg, A. *Science* **1995**, *268*, 1728–1731.
(3) Yu, S.; Azzam, T.; Rouiller, I.; Eisenberg, A. *J. Am. Chem. Soc.* **2009**, *131*, 10557–66.
(4) Zhang, L. F.; Eisenberg, A. *J. Am. Chem. Soc.* **1996**, *118*, 3168–3181.
(5) Ghoroghchian, P. P.; Li, G.; Levine, D. H.; Davis, K. P.; Bates, F. S.; Hammer, D. A.; Therien, M. J. *Macromolecules* **2006**, *39*, 1673–1675.
(6) Levine, D. H.; Ghoroghchian, P. P.; Freudenberg, J.; Zhang, G.; Therien, M. J.; Greene, M. I.; Hammer, D. A.; Murali, R. *Methods* **2008**, *46*, 25–32.
(7) Discher, D. E.; Eisenberg, A. *Science* **2002**, *297*, 967–973.
(8) Choucair, A.; Eisenberg, A. *Eur. Phys. J. E* **2003**, *10*, 37–44.
(9) Discher, D. E.; Ahmed, F. *Annu. Rev. Biomed. Eng.* **2006**, *8*, 323–341.
(10) Sundararaman, A.; Stephan, T.; Grubbs, R. B. *J. Am. Chem. Soc.* **2008**, *130*, 12264–12265.
(11) Zhao, J.; Zhang, G.; Pispas, S. *J. Polym. Sci., Part A: Polym. Chem.* **2009**, *47*, 4099–4110.
(12) Smith, A. E.; Xu, X.; Abell, T. U.; Kirkland, S. E.; Hensarling, R. M.; McCormick, C. L. *Macromolecules* **2009**, *42*, 2958–2964.
(13) Hawker, C. J.; Bosman, A. W.; Harth, E. *Chem. Rev.* **2001**, *101*, 36613688.
(14) Matyjaszeski, K.; Xia, J. *Chem. Rev.* **2001**, *101*, 2921–2990.
(15) Moad, G.; Rizzardo, E.; Thang, S. H. *Aust. J. Chem.* **2005**, *58*, 379–410.
(16) Lowe, A. B.; McCormick, C. L. *Prog. Polym. Sci.* **2007**, *32*, 283–351.
(17) McCormick, C. L.; Lowe, A. B. *Acc. Chem. Res.* **2004**, *37*, 312–325.
(18) Butun, V.; Liu, S.; Weaver, J. V. M.; Bories-Azeau, X.; Cai, Y.; Armes, S. P. *React. Funct. Polym.* **2006**, *66*, 157–165.
(19) Butun, V.; Billingham, N. C.; Armes, S. P. *J. Am. Chem. Soc.* **1998**, *120*, 11818–11819.

(20) Vo, C.-D.; Armes, S. P.; Randall, D. P.; Sakai, K.; Biggs, S. *Macromolecules* **2007**, *40*, 157–167.
(21) Wang, D.; Yin, J.; Zhu, Z.; Ge, Z.; Liu, H.; Armes, S. P.; Liu, S. *Macromolecules* **2006**, *39*, 7378–7385.
(22) Cai, Y.; Armes, S. P. *Macromolecules* **2005**, *38*, 271–279.
(23) Bories-Azeau, X.; Armes, S. P.; Van den Haak, H. J. W. *Macromolecules* **2004**, *37*, 2348–2352.
(24) Liu, S.; Armes, S. P. *Langmuir* **2003**, *19*, 4432–4438.
(25) Liu, S.; Armes, S. P. *Angew. Chem., Int. Ed.* **2002**, *41*, 1413–1416.
(26) Arotcarena, M.; Heise, B.; Ishaya, S.; Laschewsky, A. *J. Am. Chem. Soc.* **2002**, *124*, 3787–3793.
(27) Virtanen, J.; Arotcarena, M.; Heise, B.; Ishaya, S.; Laschewsky, A.; Tenhu, H. *Langmuir* **2002**, *18*, 5360–5365.
(28) Weaver, J. V. M.; Armes, S. P.; Buetuen, V. *Chem. Commun.* **2002**, 2122–2123.
(29) Wang, D.; Wu, T.; Wan, X.; Wang, X.; Liu, S. *Langmuir* **2007**, *23*, 11866–11874.
(30) Chang, C.; Wei, H.; Feng, J.; Wang, Z.-C.; Wu, X.-J.; Wu, D.-Q.; Cheng, S.-X.; Zhang, X.-Z.; Zhuo, R.-X. *Macromolecules* **2009**, *42*, 4838–4844.
(31) Zhang, Y.; Liu, H.; Hu, J.; Li, C.; Liu, S. *Macromol. Rapid Commun.* **2009**, *30*, 941–947.
(32) Jiang, X.; Zhang, G.; Narain, R.; Liu, S. *Langmuir* **2009**, *25*, 2046–2054.
(33) Zhang, Y.; Wu, T.; Liu, S. *Macromol. Chem. Phys.* **2007**, *208*, 2492–2501.
(34) Rao, J.; Luo, Z.; Ge, Z.; Liu, H.; Liu, S. *Biomacromolecules* **2007**, *8*, 3871–3878.
(35) Jiang, X.; Ge, Z.; Xu, J.; Liu, H.; Liu, S. *Biomacromolecules* **2007**, *8*, 3184–3192.
(36) Ge, Z.; Cai, Y.; Yin, J.; Zhu, Z.; Rao, J.; Liu, S. *Langmuir* **2007**, *23*, 1114–1122.
(37) Lowe, A. B.; Torrex, M.; Wang, R. *J. Polym. Sci., Part A: Polym. Chem.* **2004**, *45*, 5864–5871.
(38) Butun, V.; Top, R. B.; Ufuklar, S. *Macromolecules* **2006**, *39*, 1216–1225.
(39) Convertine, A. J.; Benoit, D. S. W.; Duvall, C. L.; Hoffman, A. S.; Stayton, P. S. *J. Contolled Release* **2009**, *133*, 221–229.
(40) Liang, W.-J.; Lien, C.-H.; Kuo, P.-L. *J. Colloid Interface Sci.* **2006**, *294*, 371–375.
(41) Adams, D. J.; Armes, S. P.; Weaver, A. C. *Langmuir* **2006**, *22*, 4534–4540.
(42) Convertine, A. J.; Lokitz, B. S.; Vasileva, Y.; Myrick, L. J.; Scales, C. W.; Lowe, A. B.; McCormick, C. L. *Macromolecules* **2006**, *39*, 1724–1730.
(43) Magenau, A. J. D.; Martinez-Castro, N.; Savin, D. A.; Storey, R. F. *Macromolecules* **2009**, *42*, 8044–8051.
(44) Burchard, W. *Adv. Polym. Sci.* **1983**, *48*, 1–124.
(45) Dou, H. J.; Jiang, M.; Peng, H. S.; Chen, D. Y.; Hong, Y. *Angew. Chem., Int. Ed.* **2003**, *42*, 1516–1519.
(46) Wan, W.-M.; Sun, X.-L.; Pan, C.-Y. *Macromolecules* **2009**, *42*, 4950–4952.
(47) Kujawa, P.; Segui, F.; Shaban, S.; Diab, C.; Okada, Y.; Tanaka, F.; Winnik, F. M. *Macromolecules* **2006**, *39*, 341–348.
(48) Xia, Y.; Yin, X. C.; Burke, N. A. D.; Stover, H. D. H. *Macromolecules* **2005**, *38*, 5937–5943.